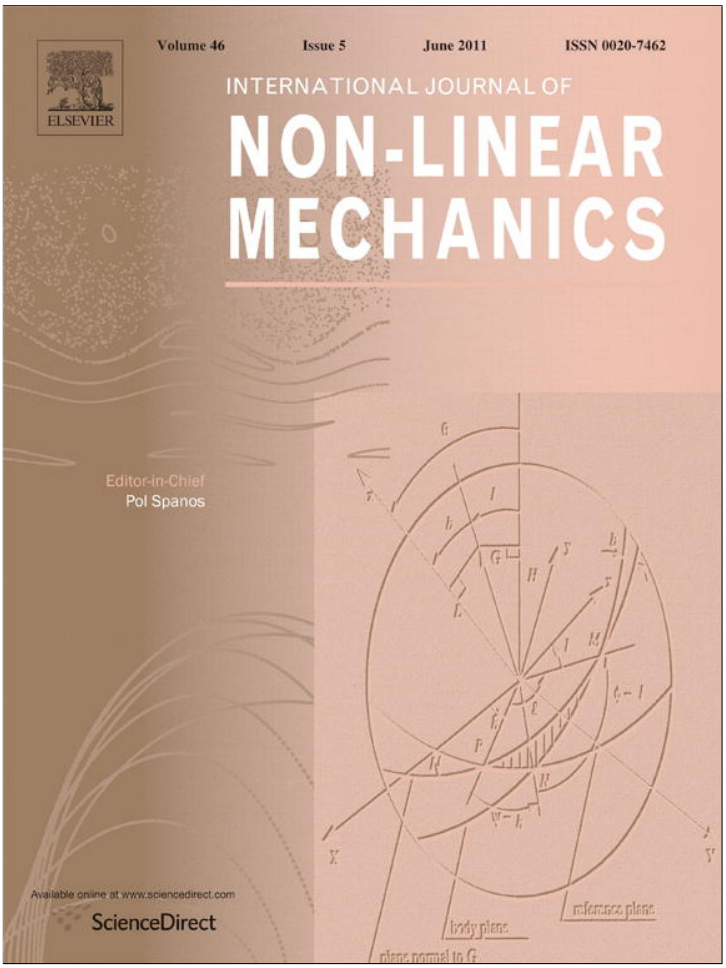

International Journal of Non-Linear Mechanics 46 (2011) 703–710

Contents lists available at ScienceDirect

International Journal of Non-Linear Mechanics

journal homepage: www.elsevier.com/locate/nlm

Non-linear principal resonance of an orthotropic and magnetoelastic rectangular plate

C.X. Xue [a,b], E. Pan [b,*], Q.K. Han [b,c], S.Y. Zhang [d], H.J. Chu [b,e]

[a] Department of Mechanics, College of Science, North University of China, Taiyuan 030051, P.R. China
[b] Department of Civil Engineering, University of Akron, Akron, OH 44325, USA
[c] School of Mechanical Engineering and Automation, Northeastern University, Shenyang, 110004, P.R. China
[d] Institute of Applied Mechanics, Taiyuan University of Technology, Taiyuan 030024, P.R. China
[e] College of Hydraulic Science and Engineering, Yangzhou University, Yangzhou 225009, P.R. China

ARTICLE INFO

Article history:
Received 12 July 2010
Received in revised form
29 November 2010
Accepted 13 February 2011
Available online 21 February 2011

Keywords:
Orthotropic plate
Large deflection
Magnetoelasticity
Non-linear principal resonance
Stability
Multiple-scale method

ABSTRACT

Based on the von Karman plate theory of large deflection, we have derived a non-linear partial differential equation for the vibration of a thin orthotropic plate under the combined action of a transverse magnetic field and a transverse harmonic mechanical load. The influence of the magnetic field is due to the magnetic Lorentz force induced by the eddy current. By employing the Bubnov–Galerkin method, the non-linear partial differential equation is transformed into a third-order non-linear ordinary differential equation. The amplitude-frequency equations are further derived by means of the multiple-scale method. As numerical examples for an orthotropic plate made of silver, the influence of the magnetic field, orthotropic material property, plate thickness, and the mechanical load on the principal resonance behavior is investigated. The higher-order effect and stability of the solution are also discussed.

1. Introduction

Magnetoelastic (ME) structures have been widely used in various high technology apparatus and equipments. Due to the inherent non-linear characteristics and the multi-physics coupling effect in these structures, certain complicated static and dynamic phenomena have been observed [1,2]. The ME structure often experiences large deformation and vibration when a strong magnetic field and/or mechanical excitation are applied during the process of manufacturing or when the structure is in service. Since the ME plate plays a significant role in these structures, it is crucial to understand its non-linear vibration characteristics.

For a thin plate under large deformation, Nayfeh and Mook [3], Sathyamoorthy [4], and Yang and Sethna [5] studied the non-linear dynamic behavior of isotropic plates under various parametric loadings. Nayfeh and Pai [6] investigated the planar and non-planar responses of a non-extensional cantilever beam, and found that the hardening effect and non-planar responses for all modes were due to the non-linear geometric terms involved. Furthermore, vibration of orthotropic plates resting on elastic foundations with classical boundary conditions and elastically restrained edges was thoroughly analyzed [7,8]. Moorthy et al. [9] investigated the parametric instability of laminated composite plates with transverse shear deformation subjected to uniaxial harmonic loading using the finite element method. Udar and Datta [10] studied the resonance characteristics of simply supported laminated square plates subjected to non-uniform and concentrated edge loading. Shih and Bloter [11] analyzed the non-linear vibration of laminated thin rectangular plates on an elastic foundation and discussed the influence of the excitation amplitude, material lamination, and boundary conditions on its non-linear frequency. Hsu [12] studied the vibration response of orthotropic plates on non-linear elastic foundations using the differential quadrature method.

With regard to the non-linear analysis of magnetoelastic structures, Moon and Pao [13], and Pao and Yeh [14] studied the magnetoelastic vibration of a ferromagnetic cantilever beam under a magnetic field. Recently, Hasanyan et al. [15] proposed a mathematical model for the non-linear vibration of a conductive plate under an inclined magnetic field. Librescu et al. [16] studied the geometric non-linearity of elastic isotropic plates subjected to an external magnetic field. Belubekyan et al. [17] presented the magnetoelastic vibration of a flat plate immersed in an external magnetic field and found that the localized bending vibration can be eliminated by means of an applied magnetic field. Hu et al. [18]

* Corresponding author. Tel.: +1 330 972-6739; fax: +1 330 972-6020.
E-mail addresses: maryxue2010@gmail.com (C.X. Xue), pan2@uakron.edu (E. Pan), qhan@mail.neu.edu.cn (Q.K. Han), syzhang@tyut.edu.cn (S.Y. Zhang), hjchu@yzu.edu.cn (H.J. Chu).

0020-7462/$ - see front matter © 2011 Elsevier Ltd. All rights reserved.
doi:10.1016/j.ijnonlinmec.2011.02.002

studied the non-linear magnetoelastic vibration of a current-conducting thin plate under a magnetic field. Gao and Qi [19] obtained the magneto-elastic-plastic response of a ferromagnetic beam-plate under magnetic pulses. Pratiher and Dwivedy [20] studied the non-linear dynamics of a soft magneto-elastic manipulator with large transverse deflection under a time varying magnetic field and a harmonic (mechanical) excitation.

Until now, there are very few published literature on the non-linear vibration behaviors of a magnetoelastic plate, especially with consideration of both its orthotropic characteristics and the magnetic loading. In this paper, therefore, we study the non-linear principal resonances of an orthotropic magnetoelastic plate under a transverse magnetic field and a mechanical force using the multi-scale method based on the perturbation approach [21]. First, based on the von Karman's orthotropic plate theory of large deflection and the introduced magnetic Lorentz force, we derive the mathematical model. Then, the amplitude-frequency response equation in the steady state is obtained by means of the multiple scale method. The principle resonance of the plate made of silver and an isotropic material is analyzed. Numerical results show clearly the influence of the magnetic field, material property, plate thickness, and external force amplitudes on the principle resonance. The higher-order effect and stability of the solution are also discussed.

2. Plate model and governing equations

2.1. Description of a general plate model with ME effect

We consider a simply supported, rectangular, and orthotropic magnetoelastic thin plate, as shown in Fig. 1. The length, width, and thickness of the plate are L_x, L_y, and h, respectively. The coordinate plane Oxy is attached to the middle plane of the plate with its z-axis normal to it. The plate is under a constant magnetic field $\boldsymbol{B}(0, 0, B_z)$ and a time-harmonic mechanical load $q(t)$ in z-direction.

The constitutive relations for an orthotropic plate are

$$\sigma_x = E_x\varepsilon_x + E_{xy}\varepsilon_y,\ \sigma_y = E_{xy}\varepsilon_x + E_y\varepsilon_y,\ \tau_{xy} = G\gamma_{xy} \tag{1}$$

where E_x, E_y, E_{xy}, and G are the material coefficients.

We derive the governing equation by following the thin-plate theory [22]. However, in order to include the in-plane force effect, the non-linear terms in the equations of motion involving products of the stress and plate slope are retained, and all other non-linear terms are neglected. Based on the von Karman's plate theory of large deflection [23], the Lagrangian strains of the plate are

$$\varepsilon_x = \frac{\partial u}{\partial x} + \frac{1}{2}\left(\frac{\partial w}{\partial x}\right)^2,\ \varepsilon_y = \frac{\partial v}{\partial y} + \frac{1}{2}\left(\frac{\partial w}{\partial y}\right)^2,\ \gamma_{xy} = \frac{\partial v}{\partial x} + \frac{\partial u}{\partial y} + \frac{\partial w}{\partial x}\frac{\partial w}{\partial y} \tag{2}$$

where u, v, and w denote the displacement in the x-, y-, and z-directions, respectively.

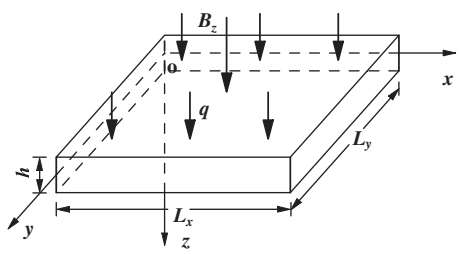

Fig. 1. Diagram of a rectangular plate under transverse magnetic field $\boldsymbol{B}$ and mechanical load q.

Taking the derivative of Eq. (2), we first obtain the strain compatibility equation as follows:

$$\frac{\partial^2\varepsilon_x}{\partial y^2} + \frac{\partial^2\varepsilon_y}{\partial x^2} - \frac{\partial^2\gamma_{xy}}{\partial x\partial y} = \left(\frac{\partial^2 w}{\partial x\partial y}\right)^2 - \frac{\partial^2 w}{\partial x^2}\frac{\partial^2 w}{\partial y^2} \tag{3}$$

We further introduce the Airy stress function φ, which satisfies

$$\sigma_x = \frac{\partial^2\varphi}{\partial y^2},\ \sigma_y = \frac{\partial^2\varphi}{\partial x^2},\ \tau_{xy} = -\frac{\partial^2\varphi}{\partial x\partial y}$$

Along with Eq. (1), Eq. (3) can be recast as

$$\frac{E_x}{E_xE_y - E_{xy}^2}\frac{\partial^4\varphi}{\partial x^4} + \left(\frac{1}{G} - \frac{2E_{xy}}{E_xE_y - E_{xy}^2}\right)\frac{\partial^4\varphi}{\partial x^2\partial y^2} + \frac{E_y}{E_xE_y - E_{xy}^2}\frac{\partial^4\varphi}{\partial y^4} = -\frac{1}{2}L(w,w) \tag{4}$$

where the non-linear operator L on the right-hand side is defined as

$$L(\alpha,\beta) = \alpha_{,xx}\beta_{,yy} + \alpha_{,yy}\beta_{,xx} - 2\alpha_{,xy}\beta_{,xy} \tag{5}$$

The displacement vector of the thin plate $\boldsymbol{u}(x,y,z,t)$ is assumed as [22]

$$\boldsymbol{u} = \left(-z\frac{\partial w}{\partial x}\right)\boldsymbol{i} + \left(-z\frac{\partial w}{\partial y}\right)\boldsymbol{j} + w(x,y,t)\boldsymbol{k} \tag{6}$$

Due to the magneto-electric property of the ME plate, an eddy current will be induced by the relative motion between the plate and the magnetic field. Based on the Ohm's law [24], the induced current density vector of the plate is

$$\boldsymbol{J} = \sigma\left(\frac{\partial\boldsymbol{u}}{\partial t} \times \boldsymbol{B}\right) \tag{7}$$

where σ and $\boldsymbol{B}$ are, respectively, the electric conductivity and magnetic induction vector.

Therefore, the Lorenz force vector per unit area is

$$\boldsymbol{f} = \sigma\left(\frac{\partial\boldsymbol{u}}{\partial t} \times B_z\boldsymbol{k}\right) \times B_z\boldsymbol{k} = \sigma\left(zB_z{}^2\frac{\partial^2 w}{\partial x\partial t}\boldsymbol{i} + zB_z^2\frac{\partial^2 w}{\partial y\partial t}\boldsymbol{j}\right)) \equiv f_x\boldsymbol{i} + f_y\boldsymbol{j} \tag{8}$$

and the corresponding electromagnetic moments are

$$m_x = \int_{-(h/2)}^{(h/2)} f_x z dz = \frac{\sigma h^3 B_z^2}{12}\frac{\partial^2 w}{\partial x\partial t},\quad m_y = \int_{-(h/2)}^{h/2} f_y z dz = \frac{\sigma h^3 B_z^2}{12}\frac{\partial^2 w}{\partial y\partial t} \tag{9}$$

The electromagnetic moments will influence the motion of the plate in the z-direction with their equivalent magnetic force being [25]

$$F_z^e(x,y,z) = \frac{\partial m_x}{\partial x} + \frac{\partial m_y}{\partial y} = \frac{\sigma h^3 B_z{}^2}{12}\frac{\partial^3 w}{\partial x^2\partial t} + \frac{\sigma h^3 B_z{}^2}{12}\frac{\partial^3 w}{\partial y^2\partial t} \tag{10}$$

We assume also that the external excitation force as $q = q_0\cos\omega t$ in which q_0 is the amplitude and ω is the angular frequency. Then, by considering the inertia force and the equivalent magnetic force, the governing equation of the deflection for the orthotropic ME plate becomes

$$D_x\frac{\partial^4 w}{\partial x^4} + 2(D_{xy} + 2D_G)\frac{\partial^4 w}{\partial x^2\partial y^2} + D_y\frac{\partial^4 w}{\partial y^4} = hL(w,\varphi) - \rho h\ddot{w} + F_z^e + q_0\cos\omega t \tag{11}$$

where $D_x = E_xh^3/12$, $D_y = E_yh^3/12$, $D_{xy} = E_{xy}h^3/12$, and $D_G = Gh^3/12$ are the stiffness coefficients of the plate, and ρ is the density of the plate per unit area.

2.2. Derivation of the governing equation for a simply supported plate

For a simply supported ME plate, its lateral boundary conditions are

$$x=0 \text{ and } x=L_x:\ w=0,\ \frac{\partial^2 w}{\partial x^2}=0$$

$$y=0 \text{ and } y=L_y:\ w=0,\ \frac{\partial^2 w}{\partial y^2}=0 \tag{12}$$

By the method of variables separation, the transverse displacement w can be assumed as

$$w(x,y,t)=T(t)\sin\left(\frac{m\pi x}{L_x}\right)\sin\left(\frac{n\pi y}{L_y}\right) \tag{13}$$

where m and n are both positive integers denoting different modes of the plate, and $T(t)$ is the amplitude of w.

Substituting Eq. (13) into Eq. (4), we find the Airy function of the plate in the following form:

$$\varphi=\frac{1}{32}T^2(t)\left[\frac{E_xE_y-E_{xy}^2}{E_x}\left(\frac{nL_x}{mL_y}\right)^2\cos\frac{2m\pi x}{L_x}+\frac{E_xE_y-E_{xy}^2}{E_y}\left(\frac{mL_y}{nL_x}\right)^2\cos\frac{2n\pi y}{L_y}\right] \tag{14}$$

Furthermore, if we substitute Eqs. (10), (13), and (14) into the governing equation of the plate, i.e. Eq. (11), we obtain

$$\left[\rho h\ddot{T}(t)+\kappa_1\dot{T}(t)+\kappa_2T(t)+\kappa_3T^3(t)\right]\sin\frac{m\pi x}{L_x}\sin\frac{n\pi y}{L_y}=q_0\cos\omega t \tag{15}$$

where

$$\kappa_1=\frac{\sigma h^3B_z^2}{12}\left[\left(\frac{m\pi}{L_x}\right)^2+\left(\frac{n\pi}{L_y}\right)^2\right]$$

$$\kappa_2=D_x\left(\frac{m\pi}{L_x}\right)^4+2(D_{xy}+2D_G)\left(\frac{m\pi}{L_x}\right)^2\left(\frac{n\pi}{L_y}\right)^2+D_y\left(\frac{n\pi}{L_y}\right)^4$$

$$\kappa_3=\frac{h}{8}\left(\frac{m\pi}{L_x}\right)^4\frac{E_xE_y-E_{xy}^2}{E_y}\cos\frac{2n\pi y}{L_y}+\frac{h}{8}\left(\frac{n\pi}{L_y}\right)^4\frac{E_xE_y-E_{xy}^2}{E_x}\cos\frac{2m\pi x}{L_x}$$

After applying the Bubnov–Galerkin method to Eq. (15) and integrating the result over the whole plate area, we obtain

$$\rho h\ddot{T}(t)+\kappa_1\dot{T}(t)+\kappa_2T(t)+\kappa_4T^3(t)=\frac{16q_0}{\pi^2}\cos\omega t \tag{16}$$

where

$$\kappa_4=\frac{3}{4h^2}\left[\left(\frac{m\pi}{L_x}\right)^4\frac{D_xD_y-D_{xy}^2}{D_y}+\left(\frac{n\pi}{L_y}\right)^4\frac{D_xD_y-D_{xy}^2}{D_x}\right]$$

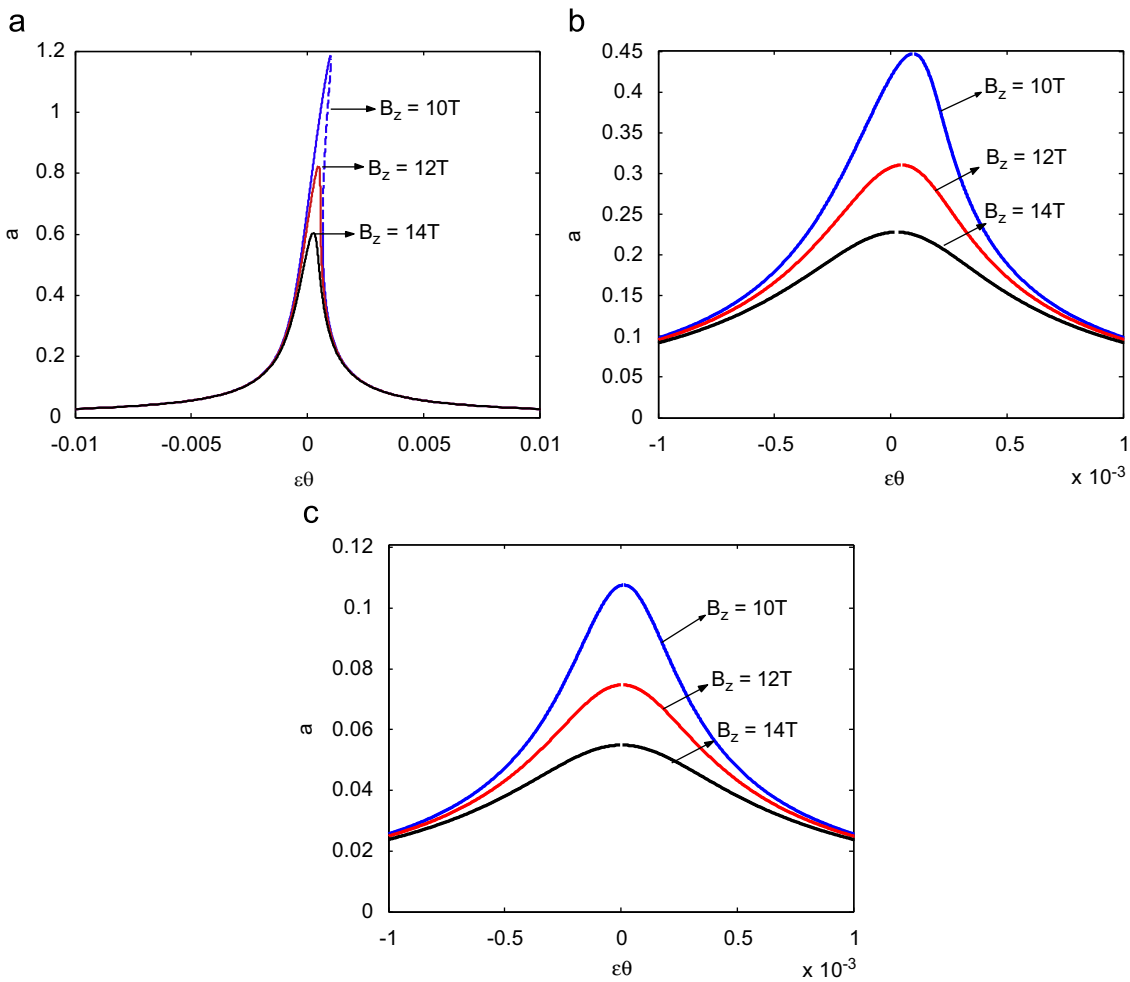

Fig. 2. Frequency response of the principal resonance of the orthotropic plate under different magnetic induction B_z for three modes (h=1.0 mm, q_0=0.01 MPa, ε=0.01): (m,n)=(1,1) in (a), (m,n)=(2,1) in (b), and (m,n)=(1,2) in (c).

We now introduce the following dimensionless parameters/variables: $\tau=\omega_0 t$, $\omega_0=\sqrt{\kappa_2/\rho h}$, $\overline{\omega}=\omega/\omega_0$, $f=T/h$, $\dot{f}=df/d\tau$, and $\ddot{f}=d^2f/d\tau^2$.

with ω_0 being the natural frequency of the system. Then the non-dimensional governing equation of the plate becomes the Duffing-type equation with hard-spring characteristics:

$$\ddot{f}(\tau)+\delta\dot{f}(\tau)+f(\tau)+\alpha_3 f^3(\tau)=K\cos\overline{\omega}\tau \tag{17}$$

with

$$\delta=\frac{\sigma h^2 B_z^2}{12\rho\omega_0}\left[\left(\frac{m\pi}{L_x}\right)^2+\left(\frac{n\pi}{L_y}\right)^2\right] \tag{18a}$$

$$\alpha_3=\frac{3}{4\rho h\omega_0^2}\left[\left(\frac{m\pi}{L_x}\right)^4\frac{D_xD_y-D_{xy}^2}{D_y}+\left(\frac{n\pi}{L_y}\right)^4\frac{D_xD_y-D_{xy}^2}{D_x}\right] \tag{18b}$$

$$K=\frac{16q_0}{\rho\pi^2\omega_0{}^2h^2} \tag{18c}$$

where δ is the effective damping coefficient, α_3 is the coefficient of the cubic non-linearity, and K is the amplitude of the equivalent excitation.

3. Principal resonance of the ME plate

3.1. Amplitude-frequency response of the ME plate

To solve Eq. (17), we employ the method of multiple scales [3,26]. For the principle resonance analysis, the excitation frequency is close to the linear natural frequency of the system, i.e. $\omega\approx\omega_0$. We assume that if $K=O(\varepsilon)$ where $\varepsilon\ll 1$, then $f=O(1)$. We further assume that both the damping and non-linearity terms to be in the order of $O(\varepsilon)$. Then, the magnitude ordering can be derived from Eq. (17) as in the following form:

$$\ddot{f}+f=-\varepsilon\alpha_3 f^3-\varepsilon\delta\dot{f}+\varepsilon K\cos\overline{\omega}\tau \tag{19}$$

The first asymptotic solution of this equation can be assumed as

$$f(t,\varepsilon)=f_0(T_0,T_1)+\varepsilon f_1(T_0,T_1)+O(\varepsilon^2) \tag{20}$$

where $T_0=t$ and $T_1=\varepsilon t$ are the fast and slow time-scales, respectively; and f_0 and f_1 are unknown functions to be determined. Since $\omega\approx\omega_0$, we can assume

$$\overline{\omega}=1+\varepsilon\theta \tag{21}$$

where θ is the detuning parameter and ε again is a small perturbation variable.

We now substitute Eqs. (20) and (21) into Eq. (19). Letting the coefficients of the like powers of ε to be zero, we find the following equations for different orders. To order ε^0, we have

$$D_0^2 f_0+f_0=0 \tag{22a}$$

and to order ε^1, we have

$$D_0^2 f_1+f_1=-2D_0D_1f_0+K\cos\overline{\omega}T_0-\delta D_0 f_0-\alpha_3 f_0^3 \tag{22b}$$

where $D_n=\partial/\partial T_n$ $(n=0,1)$ denotes the partial differential operator.

We assume the general solution of Eq. (22a) as

$$f_0=A(T_1)e^{iT_0}+\overline{A}(T_1)e^{-iT_0} \tag{23}$$

Then, substituting this equation into Eq.(22b) gives

$$D_0^2 f_1+f_1=\left(\tfrac{1}{2}Ke^{i\theta T_1}-i2A'-3\alpha_3A^2\overline{A}-i\delta A\right)e^{iT_0}-\alpha_3A^3e^{i3T_0}+cc \tag{24}$$

where cc denotes the complex conjugate of the preceding terms. In order to eliminate the secular terms in f_1, we let

$$\tfrac{1}{2}Ke^{i\theta T_1}-i2A'-3\alpha_3A^2\overline{A}-i\delta A=0 \tag{25}$$

Then the solution of Eq. (24) can be found as

$$f_1=\frac{\alpha_3}{8}A^3e^{i3T_0}+cc \tag{26}$$

Assuming $A=ae^{i\varphi}/2$, $a(T_1),\phi(T_1)\in R$, and substituting it into Eq. (25), upon further separating its real and imaginary parts of the result, we derive the following pair of modulation equations:

$$\begin{cases}\frac{da}{dT_1}=-\frac{\delta}{2}a+\frac{K}{2}\sin\beta\\ a\frac{d\beta}{dT_1}=\theta\,a-\frac{3\alpha_3}{8}a^3+\frac{K}{2}\cos\beta\end{cases} \tag{27}$$

where $\beta=\theta T_1-\phi$. The amplitude-frequency response equation in the steady state can be obtained by assuming $da/dT_1=0$ and $d\beta/dT_1=0$, with the result being

$$\left[\frac{\varepsilon^2\delta^2}{4}+\left(\varepsilon\theta-\varepsilon\frac{3\alpha_3}{8}a^2\right)^2\right]a^2=\frac{\varepsilon^2K^2}{4} \tag{28}$$

We point out that higher-order asymptotic solution of f can be also found by following a similar procedure [27]. For instance, the second-order asymptotic solution of f can be assumed as

$$f(\tau,\varepsilon)=f_0(T_0,T_1,T_2)+\varepsilon f_1(T_0,T_1,T_2)+\varepsilon^2 f_2(T_0,T_1,T_2)+O(\varepsilon^3) \tag{29}$$

where $T_0=\tau$, $T_1=\varepsilon\tau$, and $T_2=\varepsilon^2\tau$ are independent time-scales, and f_0, f_1 and f_2 are the unknown functions to be determined.

After some tedious but straightforward derivations, the second-order amplitude-frequency response equation in the steady state can be obtained. Actually, by assuming $da/d\tau=0$, $d\beta/d\tau=0$ (where $d/d\tau=D_0+\varepsilon D_1+\varepsilon^2D_2+O(\varepsilon^3)$), we derive the following pair of modulation equations:

$$\left(1-\frac{9}{16}\varepsilon\alpha_3a^2-\frac{\varepsilon\theta}{2}\right)K\sin\beta+\frac{\delta\varepsilon}{4}K\cos\beta=\delta a-\frac{3}{8}\varepsilon\alpha_3\delta a^3 \tag{30a}$$

$$\left(\frac{3}{16}\varepsilon\alpha_3a^2+\frac{\varepsilon\theta}{2}-1\right)K\cos\beta+\frac{\delta\varepsilon}{4}K\sin\beta=2a\theta-\frac{3}{4}\alpha_3a^3+\frac{\delta^2a\varepsilon}{4}+\frac{15}{128}\varepsilon a^5\alpha_3^2 \tag{30b}$$

After eliminating the phase β, we obtain the following higher-order (or second-order) expression:

$$K^2=\left(\frac{1}{2}a\delta\frac{512-576\varepsilon\alpha_3a^2+123\varepsilon^2\alpha_3^2a^4+96\varepsilon^2\alpha_3a^2\theta+32\varepsilon^2\delta^2}{256-288\varepsilon\alpha_3a^2-256\varepsilon\theta+81\varepsilon^2\alpha_3^2a^4+144\varepsilon^2\alpha_3a^2\theta+64\varepsilon^2\theta^2+16\varepsilon^2\delta^2}\right)^2+\left(\frac{1}{8}a\frac{\begin{array}{c}-1104\varepsilon\alpha_3^2a^4+1536\varepsilon\alpha_3a^2\theta+1536\alpha_3a^2+135\alpha_3^3a^6\varepsilon^2+120\varepsilon^2\alpha_3^2a^4\theta+96\varepsilon^2\alpha_3a^2\delta^2\\ -4096\theta+256\theta\varepsilon^2\delta a^2+2048\varepsilon\delta^2\end{array}}{256-288\varepsilon\alpha_3a^2-256\varepsilon\theta+81\varepsilon^2\alpha_3^2a^4+144\varepsilon^2\alpha_3a^2\theta+64\varepsilon^2\theta^2+16\varepsilon^2\delta^2}\right)^2 \tag{31}$$

It can be shown numerically that if ε is relatively small (say, $\varepsilon\le 0.01$), the solution based on the first-order approximation Eq. (28) agrees well with the solution based on this second-order expression. Thus, in the following sections, we will concentrate only on the first-order solution since the second-order solution is important only when ε is relatively large.

3.2. Stability of the first-order solution

We first discuss the stability of the stationary solution. Let us assume that

$$\begin{cases} a = a_0 + a_1 \\ \beta = \beta_0 + \beta_1 \end{cases} \tag{32}$$

where a_0 and β_0 are the solutions of Eq. (27), and a_1 and β_1 are two small quantities. Substituting Eq. (32) into Eq. (27) and keeping only the first-order terms of a_1 and β_1, we find

$$\begin{cases} \frac{da_1}{dT_1} = -\frac{\delta}{2}a_1 + \frac{K}{2}\beta_1 \cos\beta_0 \\ \frac{d\beta_1}{dT_1} = \left(\frac{\theta}{a_0} - \frac{9\alpha_3}{8}a_0\right)a_1 + \left(-\frac{K}{2a_0}\sin\beta_0\right)\beta_1 \end{cases} \tag{33}$$

The stability of the stationary solution is determined by the Jacobian eigenvalues of the right-hand side of Eq. (33). Thus the Jacobian of the modulation Eq. (27) becomes

$$\begin{vmatrix} -\frac{\delta}{2} - \lambda & -\left(\theta a_0 - \frac{3\alpha_3}{8}a_0^3\right) \\ \frac{\theta}{a_0} - \frac{9\alpha_3}{8}a_0 & -\frac{\delta}{2} - \lambda \end{vmatrix} = 0 \tag{34}$$

This gives

$$\lambda^2 + \delta\lambda + \left(\theta - \frac{3\alpha_3}{8}a_0^2\right)\left(\theta - \frac{9\alpha_3}{8}a_0^2\right) + \frac{\delta^2}{4} = 0 \tag{35}$$

Therefore, if

$$\left(\theta - \frac{3\alpha_3}{8}a_0^2\right)\left(\theta - \frac{9\alpha_3}{8}a_0^2\right) + \frac{\delta^2}{4} < 0 \tag{36}$$

then the stationary solution is unstable; otherwise the solution is stable [26].

The above analyses are for the orthotropic plate case. For the corresponding isotropic plate, we set $E_x = E_y = E/(1-\nu^2)$, $E_{xy} = \nu E/(1-\nu^2)$, and $G = 0.5E/(1+\nu)$. Therefore, the corresponding coefficients in Eq. (17) are reduced to

$$\delta = \frac{\sigma h^2 B_z^2}{12\rho\omega_0}\left[\left(\frac{m\pi}{L_x}\right)^2 + \left(\frac{n\pi}{L_y}\right)^2\right] \tag{37a}$$

$$\alpha_3 = \frac{3D_M(1-\nu^2)}{4\rho h\omega_0^2}\left[\left(\frac{m\pi}{L_x}\right)^4 + \left(\frac{n\pi}{L_y}\right)^4\right] \tag{37b}$$

$$K = \frac{16q_0}{\rho\pi^2\omega_0^2 h^2} \tag{37c}$$

where

$$\omega_0^2 = \frac{D_M}{\rho h}\left[\left(\frac{m\pi}{L_x}\right)^2 + \left(\frac{n\pi}{L_y}\right)^2\right]^2, \quad D_M = \frac{Eh^3}{12(1-\nu^2)}$$

and ν is the Poisson's ratio.

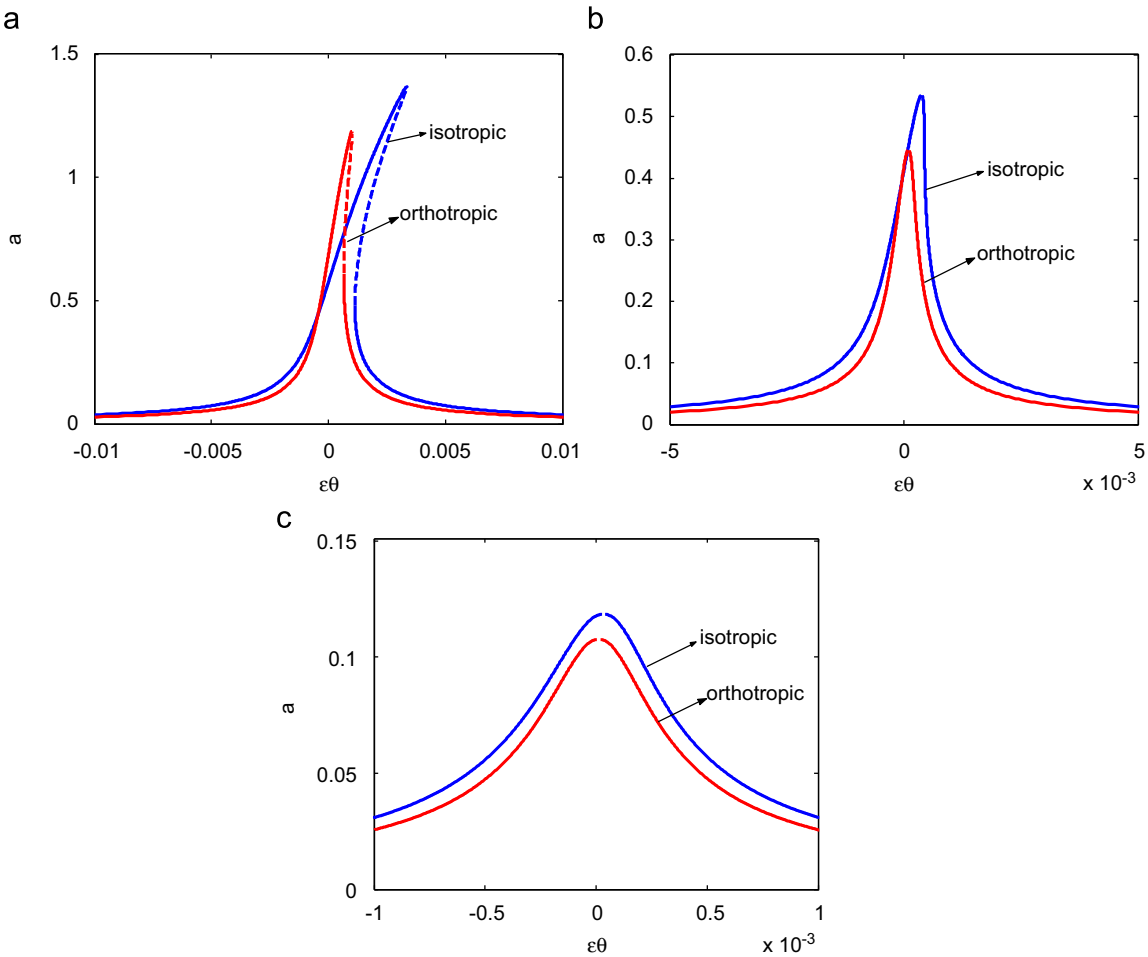

Fig. 3. Comparison of the frequency responses of the principal resonance of orthotropic and isotropic plates for three modes (h=1.0 mm, B_z=10 T, q_0=0.01 MPa, ε=0.01): (m,n)=(1,1) in (a), (m,n)=(2,1) in (b), and (m,n)=(1,2) in (c).

4. Numerical results

We first point out that when there is no magnetic induction, our solution reduces exactly to that of the corresponding purely elastic plate [26], which verifies the formulations derived in this paper. Next, the derived solutions are applied to a rectangular plate made of orthotropic (silver) or isotropic materials. The plate has the side lengths of $L_x=0.1$ m, $L_y=0.05$ m, density $\rho=10.5\times10^3$ kg/m^3, and electric conductivity $\sigma=63.0\times10^6(\Omega\,\mathrm{m})^{-1}$. The elastic moduli for silver are: $E_x=12.4\times10^{10}$ Pa, $E_y=12.4\times10^{10}$ Pa, $E_{xy}=9.34\times10^{10}$ Pa, and $G=4.61\times10^{10}$ Pa. Under the isotropic assumption, the effective elastic constants of the isotropic plate are: Young's modulus $E=11.58\times10^{10}$ Pa and Poisson's ratio $\nu=0.26$. Also in the numerical simulation, the small perturbation parameter is set to be $\varepsilon=0.01$ unless specified otherwise. The numerical results of the frequency responses of the principal resonance of the ME plate are shown in Figs. 2–6. In these figures, the dashed lines correspond to the unstable parts of the solution.

The influence of the magnetic induction B_z on the frequency response of the resonances of the orthotropic plate is shown in Fig. 2. Three different vibration modes ($(m,n)=(1,1)$; $(m,n)=(2,1)$; $(m,n)=(1,2)$) are considered. Other fixed parameters are $h=1.0$ mm and $q_0=0.01$ MPa. The typical non-linear characteristics of the Duffing system with bending hardening phenomena, including also multi-values, jump, delay, etc., are observed in the fundamental mode ($(m,n)=(1,1)$), as shown in Fig. 2a. With increase in magnetic field, the non-linear hardening is reduced (Fig. 2a). However, no obvious bending hardening effect is observed in the higher modes ($(m,n)=(2,1)$ and $(m,n)=(1,2)$), as shown in Fig. 2b and c. On the other hand, the resonance amplitude decreases with increase in magnetic induction intensity for the three modes. Actually, according to Eq. (18a), the effective damping ratio increases quadratically with the magnetic induction B_z. Therefore, the resonant amplitudes decrease significantly with increase in magnetic field. However, the width of the resonance region is not influenced. It is interesting to point out (Fig. 2) that instability of the solution appears only in the fundamental mode ($(m,n)=(1,1)$) and only when the magnetic induction B_z is relatively small ($B_z=10$ T in the example).

In Fig. 3, we compare the frequency responses of the resonance of the orthotropic plate for the three modes ($(m,n)=(1,1)$, $(2,1)$, and $(1,2)$) to those of the corresponding isotropic plate. The fixed parameters are: $h=1.0$ mm, $B_z=10$ T, and $q_0=0.01$ MPa. It is observed clearly from Fig. 3a that, for the fundamental mode (1,1), the non-linear hardening effect of the principal resonance for the isotropic plate is much stronger than that of the corresponding orthotropic silver plate where the unstable parts of the solution are also shown by dashed lines. However, material anisotropy has only very weak effect on the non-linear hardening in the higher modes (Fig. 3b and c). It is found that, for the isotropic plate case, the resonance amplitude increases slightly

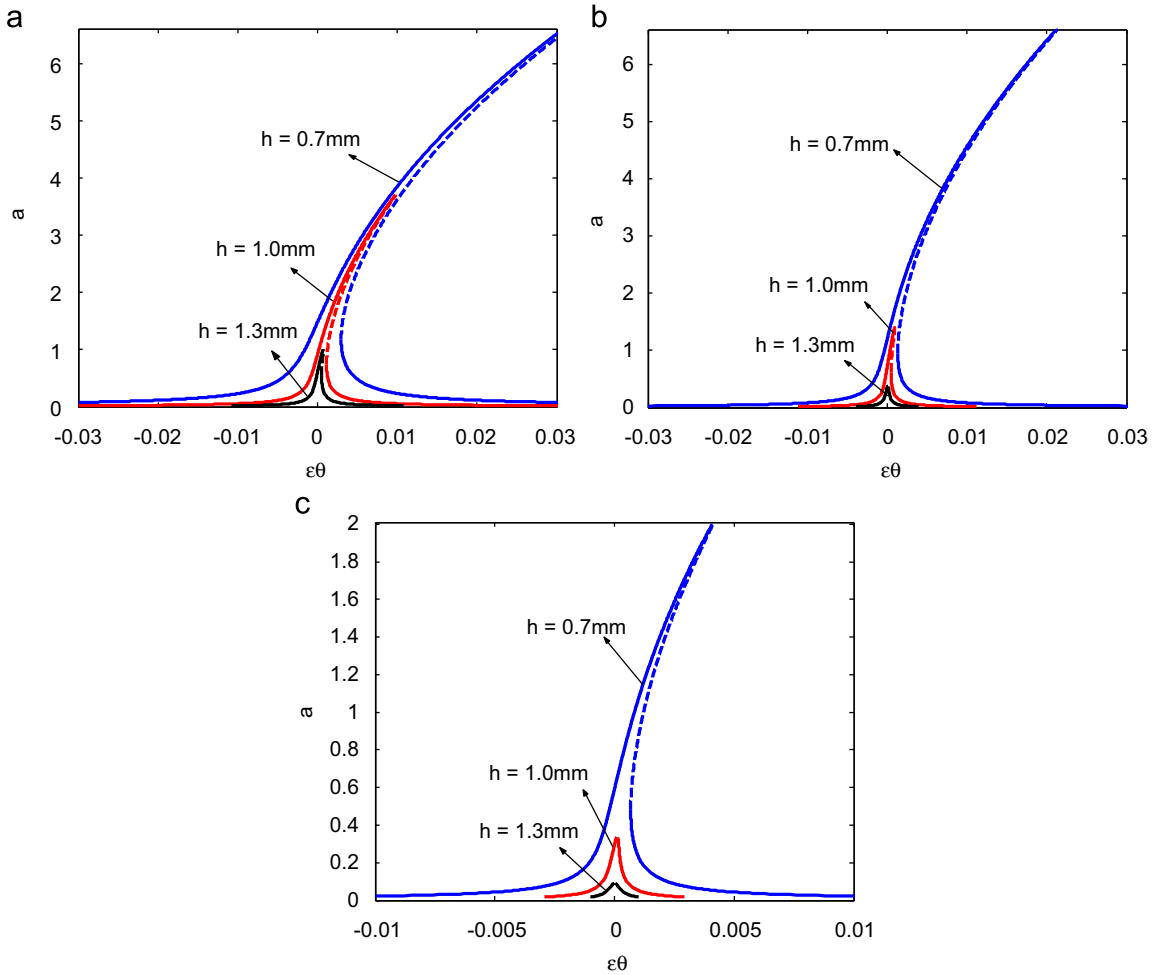

Fig. 4. Frequency response of the principal resonance of the orthotropic plate with different plate thickness h for three modes ($B_z=8$ T, $q_0=0.02$ MPa, $\varepsilon=0.01$): $(m,n)=(1,1)$ in (a), $(m,n)=(2,1)$ in (b), and $(m,n)=(1,2)$ in (c).

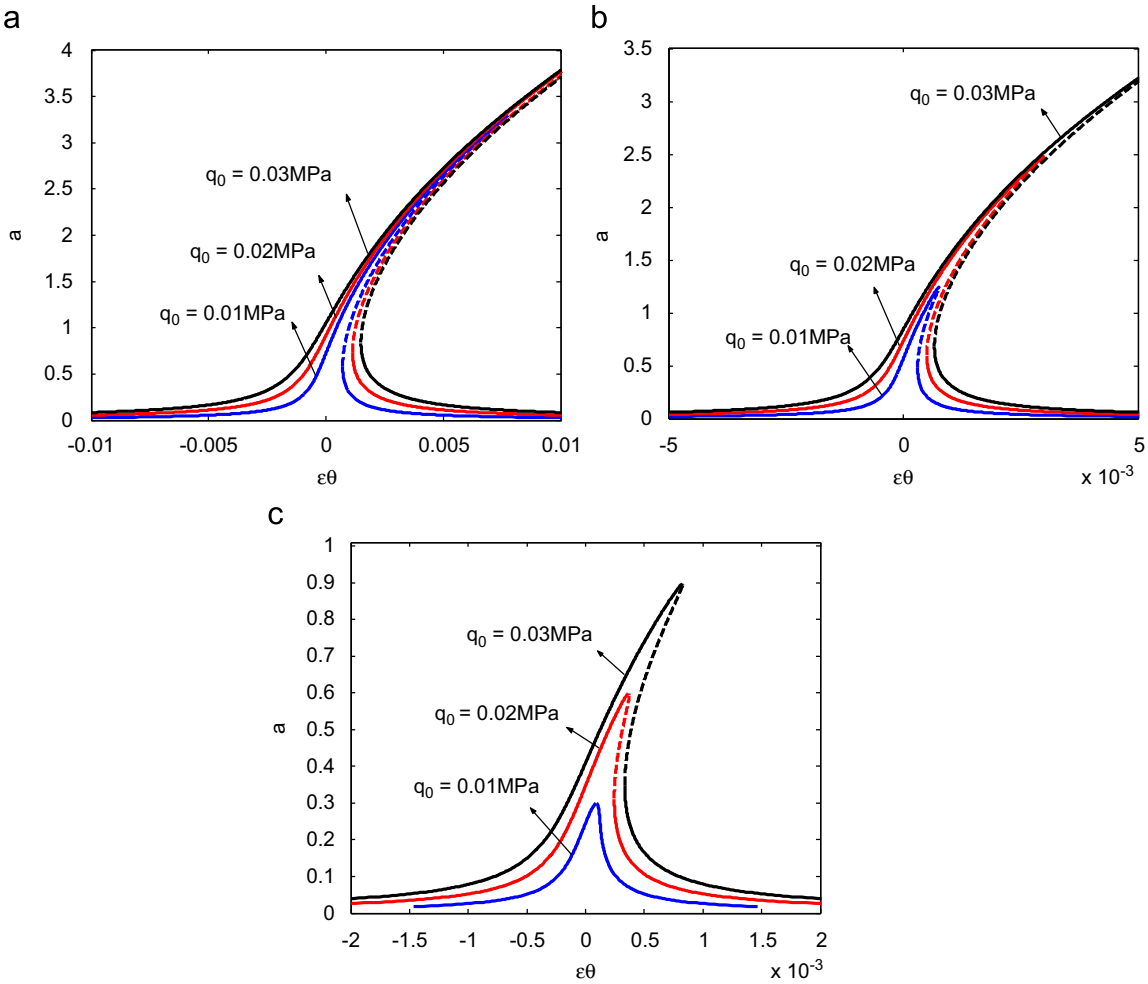

Fig. 5. Frequency response of the principal resonance of the orthotropic plate under different mechanical excitation q_0 for three modes (h=1.0 mm, B_z=6 T, ε=0.01): (m,n)=(1,1) in (a), (m,n)=(2,1) in (b), and (m,n)=(1,2) in (c).

and its width broadens as compared to the corresponding orthotropic plate case.

The effect of the plate thickness h on the frequency-amplitude response of the orthotropic plate for the three modes ((1,1), (2,1), and (1,2)) is demonstrated in Fig. 4. The fixed parameters are B_z=8 T and q_0=0.02 MPa. It is obvious from Fig. 4 that both the resonant amplitude and the non-linear bending hardening decrease with increase in plate thickness. It is also found that the widths of the resonant region become narrow in these modes with increase in plate thickness. It should be further noted that, with increase in plate thickness, the size of the unstable parts of the solutions, which appear even in the higher modes, decreases.

Fig. 5 depicts the effect of the external mechanical load q_0 on the principal resonant response of the ME plate for the three modes ((1,1), (2,1) and (1,2)). The fixed parameters are h=1.0 mm and B_z=6 T. It is clear that with decreasing mechanical load, the height of the resonance peak, and consequently the non-linear bend of the peak, decreases. This phenomenon is consistent with Eq. (17) where K in Eq. (18c) is involved. Also, the width of the resonant region shrinks when q_0 is reduced. The amplitude a in Fig. 5a is the largest among the three modes whilst the amplitude a in Fig. 5c is the smallest. The effect of the mechanical loading on the size of the unstable part of the solution, which appears in the higher modes and in the fundamental mode, can be also clearly observed.

In the numerical examples presented above, we applied the first-order solution (28) with the perturbation parameter being fixed at ε=0.01. Actually, the second-order solution (31) was also applied in the study of the principal resonance response. We found that when the perturbation parameter is small, say $\varepsilon < 0.01$, the solutions based on the first- and second-orders are

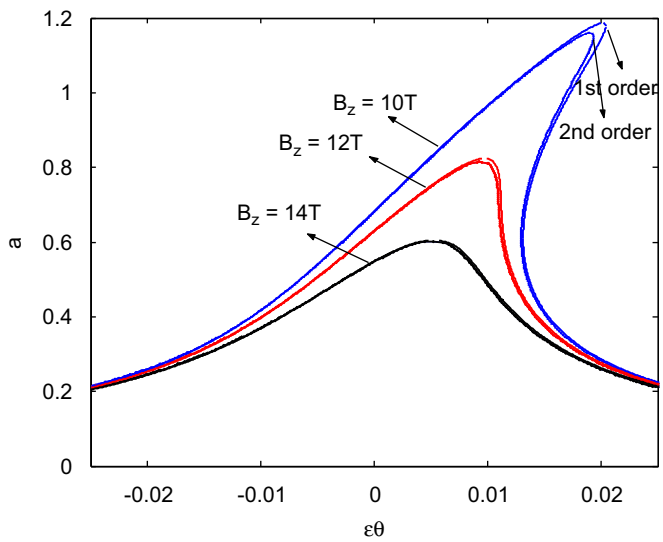

Fig. 6. Comparison of the frequency response of the principal resonance of the orthotropic plate under different magnetic induction B_z for the fundamental mode (m,n)=(1,1) (h=1.0 mm, q_0=0.01 MPa, ε=0.2): first-order vs. second-order asymptotic solutions.

undistinguishable. Even when ε is increased to 0.2, the difference between the first- and second-order solutions is only very slight. This is demonstrated in Fig. 6 for the principal resonance responses of the fundamental mode of the orthotropic plate under different magnetic induction B_z based on the first- and second-order solutions with $\varepsilon=0.2$. The other fixed parameters in this example are $h=1.0$ mm and $q_0=0.01$ MPa.

5. Conclusions

Non-linear principal resonances of an orthotropic ME thin plate with large deflection are investigated in this paper. The governing equation of the Duffing type and its corresponding asymptotic solution based on the multiple-scale method are derived. For a plate made of orthotropic silver, the influence of the applied magnetic field, plate modes, thickness, and external force is demonstrated. It is found that the amplitude of the principal resonance can be greatly affected by the magnetic-field-induced damping force. Furthermore, by carrying out a comparison study between the isotropic and the orthotropic plates, we demonstrated that it is possible to tune the principal resonance via material anisotropy of the ME plate. Stability of the solution and different orders of approximation are also discussed. These significant and interesting features will be useful in the analysis and design of magnetoelastic-related structures.

Acknowledgment

The work is supported by the National Natural Science Foundation of China (10772129) and the Science Foundation of North University of China (2009). The authors would also like to thank the two reviewers for their constructive suggestions/comments on the manuscript.

References

[1] F.C. Moon, Magneto-Solid Mechanics, John Wiley, New York, 1984.
[2] A.C. Eringen, G.A. Maugin, Electrodynamics of Continua Media, Springer, New York, 1990.
[3] A.H. Nayfeh, D.T. Mook, Nonlinear Oscillation, Wiley-Interscience, New York, 1979.
[4] M. Sathyamoorthy, Nonlinear vibration analysis of plates: a review and survey of current developments, ASME Applied Mechanics Reviews 40 (1987) 1553–1561.
[5] X.L. Yang, P.R. Sethna, Local and global bifurcations and parametrically excited vibrations of nearly square plates, International Journal of Non-Linear Mechanics 26 (1991) 199–220.
[6] A.H. Nayfeh, P.F. Pai, Non-linear non-planar parametric responses of an inextensional beam, International Journal of Non-Linear Mechanics 24 (1989) 139–158.
[7] M.H. Omurtag, F. Kadioglu, Free vibration analysis of orthotropic plates resting on Pasternak foundation by mixed finite element formulation, Computers & Structure 67 (1998) 253–265.
[8] J.N. Reddy, Mechanics of Laminated Composite Plates and Shells: Theory and Analysis, CRC Press, New York, 2004.
[9] J. Moorthy, J.N. Reddy, R.H. Plaut, Parametric instability of laminated composite plates with transverse shear deformation, International Journal of Solids and Structures 26 (1990) 801–811.
[10] R.S. Udar, P.K. Datta, Combination resonance characteristics of laminated composite plates subjected to nonuniform harmonic edge loading, Aircraft Engineering and Aerospace Technology 78 (2006) 107–119.
[11] Y.S. Shih, P.T. Bloter, Nonlinear vibration analysis of arbitrarily laminated thin rectangular plates on the elastic foundation, Journal of Sound and Vibration 167 (1993) 433–459.
[12] M.H. Hsu, Vibration analysis of orthotropic rectangular plates on elastic foundations, Composite Structures 92 (2010) 844–852.
[13] F.C. Moon, Y.H. Pao, Magnetoelastic buckling of a thin plate, ASME Journal of Applied Mechanics 35 (1968) 53–58.
[14] Y.H. Pao, C.S. Yeh, A linear theory for soft ferromagnetic elastic bodies, International Journal of Engineering Science 11 (1973) 415–436.
[15] D.J. Hasanyan, G.M. Khachaturyan, G.T. Piliposyan, Mathematical modeling and investigation of nonlinear vibration of perfectly conductive plates in an inclined magnetic field, Thin-Walled Structures 39 (2001) 111–123.
[16] L. Librescu, D. Hasanyan, D.R. Ambur, Electromagnetically conducting elastic plates in a magnetic field: modeling and dynamic implications, International Journal of Non-Linear Mechanics 39 (2004) 723–739.
[17] M. Belubekyan, K. Ghazaryan, P. Marzocca, C. Cormier, Localized magnetoelastic bending vibration of an electroconductive elastic plate, Journal of Applied Mechanics 74 (2007) 1071–1077.
[18] Y.D. Hu, G.J. Du, J. Li, Nonlinear magnetoelastic vibration analysis of current-conducting thin plate in magnetic field, in: Proceedings of Fifth International Conference on Nonlinear Mechanics, Shanghai, June 2007, pp. 631–636.
[19] Y.W. Gao, F.Q. Qi, Magneto-elastic plastic dynamic responses and instability of beam-plate excited by magnetic pulse, Journal of Vibration Engineering 20 (2007) 61–65.
[20] B. Pratiher, S.K. Dwivedy, Non-linear dynamics of a soft magneto-elastic Cartesian manipulator, International Journal of Non-Linear Mechanics 44 (2009) 757–768.
[21] A.H. Nayfeh, Introduction to Perturbation Techniques, Wiley-Interscience, New York, 1981.
[22] J.E. Ashton, J.M. Whitney, Theory of Laminated Plates, Technique Publication, U.S.A, 1970.
[23] S. Timoshenko, S. Woinowsky-Krieger, Theory of Plates and Shells, McGraw-Hill, New York, 1959.
[24] A.C. Eringen, G.A. Maugin, Electrodynamics of Continua, Springer-Verlag, New York, 1990.
[25] Y.H. Zhou, X.J. Zheng, Electromagnetic Solid Mechanics, Science Press, Beijing, 1999.
[26] J.J. Thomsen, Vibrations and Stability: Advanced Theory, and Tools, 2nd Ed., Springer-Verlag, Berlin, 2003.
[27] Z. Rahman, T.D. Burton, On higher order methods of multiple scales in non-linear oscillations—periodic steady state response, Journal of Sound and Vibration 133 (1989) 369–379.